

## On strontium and barium anomalies in the sediments of Charkadio Cave (Tilos Island, Dodekanese, Greece)

G. Steinhauser,<sup>1\*</sup> W. Hujer,<sup>2</sup> J. H. Sterba,<sup>1</sup> R. Seemann,<sup>2</sup> M. Bichler,<sup>1</sup> N. Symeonidis<sup>3</sup>

<sup>1</sup> *Atominstitut der Österreichischen Universitäten, Vienna University of Technology, Stadionallee 2, 1020 Vienna, Austria*

<sup>2</sup> *Department of Mineralogy and Petrology, Museum of Natural History Vienna, Burgring 7, 1010 Vienna, Austria*

<sup>3</sup> *Department of Historical Geology and Palaeontology, University of Athens, Panepistimiopolis, 15784 Athens, Greece*

(Received January 3, 2007)

The sediments of Charkadio Cave (Island of Tilos) have been object of chemical and mineralogical investigation. Sampling the speleothems of Charkadio Cave, it is possible to look back into the island's younger geological history. Tilos is of non-volcanic origin but neighbored to several volcanoes of the Aegean (Kos, Nisyros, and Giali). We observed a certain coincidence of increased Ba and Sr values in such samples and volcanic activity. Some of the layers of these fine-grained sediments contain volcanic particles (ash grains and lapilli). Interestingly, these strata have the highest content of Ba and Sr, as determined by neutron activation analysis. Additionally to this discovery, Sr-rich barite crystals were found in some of these layers. Thus, Ba and Sr must either exist on the surface of tephra particles in volatile and water-soluble compounds and/or were released by weathering from Ba and Sr containing feldspars (originating from pumice) in the cave sediment environment. Since other cave sediments from Tilos, which were not exposed to volcanic products, contain very much lesser quantities of Ba and Sr, we conclude that mobile Ba and Sr compounds are contributed to the sediment by volcanic fallout.

### Introduction

Tilos is an island in the Eastern Aegean Sea and part of the Dodekanese group of islands; it is located midway between Rhodes and Kos (36°27' N, 27°21' E). Tilos is mostly built of limestone and has no recent or subrecent volcanic history itself, but it is surrounded by several volcanic centers of the Aegean, in particular Kos, Nisyros, and Giali. In this study, we present the results of chemical and mineralogical investigations of the sediments of Charkadio Cave on Tilos. This cave has become famous in 1972 with the discovery of dwarf elephant bones by Nikolaos SYMEONIDIS.<sup>1</sup> This finding resulted in substantial palaeontological excavations, which are continuing since then.<sup>2–6</sup> The phenomenon of dwarfing of individual populations of mammals is not very exceptional on small islands.<sup>6–10</sup> Radiocarbon dating in the 1970s on two dwarf elephant bones from Charkadio showed an age of 4390±600 and 7090±680 years BP.<sup>3</sup> Thus, correct dating preconditioned, these dwarf elephants were the last elephants in Europe and maybe even coexisted with the early human colonization on Tilos.<sup>11</sup>

The sediments of Charkadio Cave have been object of investigation for petrological and mineralogical reasons in this study. They offer an interesting field for the investigation of cave sediments, certainly influenced by the volcanic activity of the neighboring volcanic centers. In such an environment, it is difficult to differentiate between the influence of the autochthonous relict products of limestone weathering in the frame of

karstification and the allochthonous influence of volcanic material for the total composition of the sediments. Therefore, we were looking for chemical markers that help indicate volcanic events. Precondition for this work is a fundamental knowledge about the bulk and trace element composition of volcanic eruption products.<sup>12</sup> This chemical and/or mineralogical information can even help to date the sediments approximately without using distinct tephra layers, which are used for synchronization in classic tephrochronology.<sup>13–15</sup> Tephra terms all sorts of unsolidified volcanic material like ash or pumice.

### Experimental

#### Location and sampling

The Charkadio Cave is located about 3 km south of the village Megálo Chorió, in the Mesariá Mountains, at an altitude of about 120 m above sea level. The entrance hall, about 25 by 18 m, with a basal face of approximately 300 m<sup>2</sup>, is 3 to 6 m high. The schematic section of the cave is shown in Fig. 1. An outlined ground plan of the cave can be found in Reference 3 or is available on request from the authors. The cave entrance is open in west-northwestern direction towards the mentioned volcanoes Nisyros, Giali and Kos and partly closed by huge boulders.

The cave is developed in variably bedded upper triassic bright gray limestone with inter-layerings of grey to reddish radiolarites.

\* E-mail: georg.steinhauser@ati.ac.at

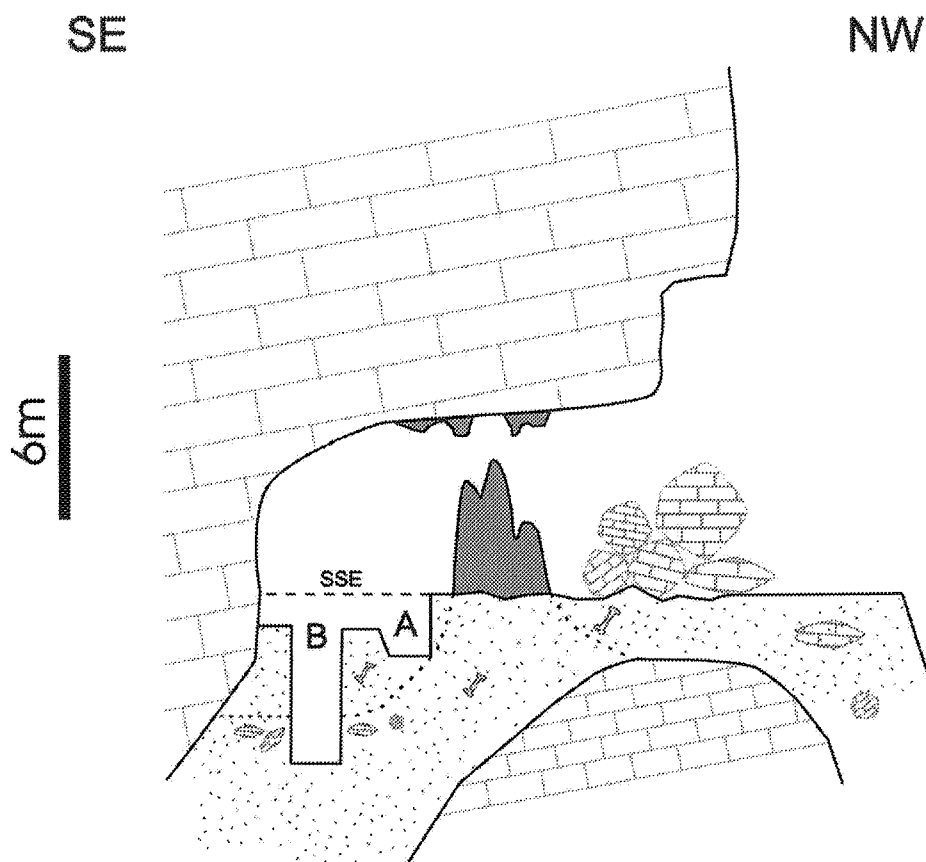


Fig. 1. Schematic section of Charkadio Cave with the two profiles that have been sampled; A: stalagmite profile; B: main profile. SSE indicates the "Sediment Surface Edge"

The cave's interior consists of debris from bedrock and heavily corroded, non active groups of big stalagmites and stalactites on the one hand. On other hand, most of the cave is filled with bright brown to gray sediments. On the sediment surface, ceramic fragments and artifacts from the younger to older history can be found. For palaeontological excavation reasons, on several positions in the cave a lot of fossil rich sediments (about 350–400 m<sup>3</sup>) have been removed. Thus it was difficult to find undisturbed sediment surface and impossible to find a complete sediment profile for adequate sampling. Therefore, two overlapping profiles were sampled, providing a stratigraphy to a depth of 5.80 m under SSE ("Sediment Surface Edge") (Fig. 1). The upper strata, including mostly undisturbed cave basement, were covered by a profile next to the stalagmites ("Stalagmite Profile", A), ranging from 0.00 to 1.90 m under SSE. The other profile ("Main Profile", B) ranges from 1.40 to a depth of 5.80 m under SSE. Thus, there is an overlap of approximately half a meter of these two profiles.

The entirety of the sediments in both profiles consists of several different stratified sequences, which were sampled every 20 cm by cutting a small brick of about 250 g out of the wall of the respective profile. Sampling was performed with utmost care with regard to bedding layers and other noteworthinesses.

The fact that fossil bones and potsherds can be found in Charkadio Cave indicates that it must have been open to the atmosphere for a longer time. It was, therefore, also exposed to the products of volcanic eruptions from the neighbored volcanic centers, especially Kos, Nisyros, and Giali.<sup>16–22</sup> The sediments, therefore, consist of a mixture of several geological and biogenic autochthonous and allochthonous relict components: karst sediments and radiolarites as residue of dissolution, more or less weathered limestone and sinter fragments, tephra and its weathering products, and karst soil ("terra rossa") from the surface, as well the fossil bones (mainly dwarf elephant, aside deer and turtle).

Additionally to Charkadio Cave, other cave sediments on Tilos ("Spider Cave") have been sampled.

The respective cave was recently opened during road constructions on the south-eastern part of the island. In contrast to Charkadio Cave, this small cave had definitely not been exposed to volcanic products. Thus the small amount of sediments found there can be regarded as the more or less pure autochthonous sediments produced by corrosion of the native carbonaceous bedrock, only with a minimum of surface material.

### INAA

Bulk analyses of the samples were performed using instrumental neutron activation analysis (INAA). Some 50 g of each sample were homogenized using an agate mortar and dried in a drying cabinet (110 °C) to constant weight. The samples were weighed into Suprasil™ quartz glass vials, sealed, and irradiated for 35 hours in the central irradiation tube of the TRIGA Mark II research reactor of the Atominstitut (Vienna University of Technology) at a thermal neutron flux of  $1 \cdot 10^{13} \text{ n} \cdot \text{cm}^{-2} \cdot \text{s}^{-1}$  together with a set of reference materials, namely CANMET reference soil SO1, NIST SRM 1633b Coal Fly Ash, Light Sandy Soil BCR No. 142, NIST SRM 2702 Inorganics in Marine Sediment, and MC Rhyolite GBW 07113 for quantification. Elemental concentrations of the samples were obtained by comparison with the certified values of these reference materials.<sup>23</sup>

After a decay time of 5 days, a first  $\gamma$ -spectrum was measured to obtain the activities of the short and medium-lived activation products  $^{24}\text{Na}$ ,  $^{42}\text{K}$ ,  $^{76}\text{As}$ ,  $^{140}\text{La}$ ,  $^{153}\text{Sm}$ , and  $^{239}\text{Np}$  (U). Three weeks later, a second measurement was started to detect the long-lived activation products  $^{46}\text{Sc}$ ,  $^{51}\text{Cr}$ ,  $^{59}\text{Fe}$ ,  $^{60}\text{Co}$ ,  $^{65}\text{Zn}$ ,  $^{85}\text{Sr}$ ,  $^{86}\text{Rb}$ ,  $^{95}\text{Zr}$ ,  $^{124}\text{Sb}$ ,  $^{131}\text{Ba}$ ,  $^{134}\text{Cs}$ ,  $^{141}\text{Ce}$ ,  $^{147}\text{Nd}$ ,  $^{152}\text{Eu}$ ,  $^{160}\text{Tb}$ ,  $^{169}\text{Yb}$ ,  $^{177}\text{Lu}$ ,  $^{181}\text{Hf}$ ,  $^{182}\text{Ta}$ , and  $^{233}\text{Pa}$  (Th). The measuring times were 1,800 seconds and 10,000 seconds, respectively. All samples were measured using an automatic sample changer with a fixed measurement position at a distance of 4 cm from the detector. The whole analysis was performed with a 222 cm<sup>3</sup> HPGe  $\gamma$ -detector (1.78 keV resolution at the 1332 keV  $^{60}\text{Co}$  peak; 48.2% relative efficiency), connected to a PC-based multi-channel analyzer with preloaded filter and Loss-Free Counting system.<sup>24,25</sup>

Values for Sr and Ba in this paper were obtained by INAA. The nuclear reaction for the production of  $^{131}\text{Ba}$  ( $T_{1/2}=11.50 \text{ d}$ ) was  $^{130}\text{Ba}(n,\gamma)^{131}\text{Ba}$ . Ba can be determined quite sensitively with INAA using its 496.33 keV  $\gamma$ -ray with an overall error of less than 5%. The detection limit of Ba in such a matrix is 20 mg/kg. The nuclear reaction used for determination of  $^{85}\text{Sr}$  ( $T_{1/2}=64.84 \text{ d}$ ) was  $^{84}\text{Sr}(n,\gamma)^{85}\text{Sr}$ . In some matrices, Sr cannot be determined sensitively, because of the

514.01 keV  $\gamma$ -ray of  $^{85}\text{Sr}$ , which can be overlapped by the 511 keV annihilation peak. In our  $\gamma$ -detection system, energy resolution was high enough for reliable quantification of Sr. Analytical errors (<10%) were higher than in case of Ba and the detection limit (15 mg/kg) was comparable to Ba.

### Mineralogical investigation

30 samples of the cave sediment were analyzed for grain size, mineralogy and heavy mineral distribution. A representative amount of each sample was ground and measured with X-ray diffractometry (Siemens D5000; Cu  $K_{\alpha}$  radiation with 40 mA/40 kV, sample rotation between 2 and 65° 2 $\theta$ ). For grain size analysis, 100 g of each sample were suspended in 10%  $\text{H}_2\text{O}_2$ . The samples were then sieved using 8, 4, 2, 1, 0.5, 0.25, 0.125 and 0.063 mm mesh sieves. Heavy minerals were separated from the 0.125–0.063 mm fraction using  $\text{C}_2\text{H}_2\text{Br}_4$  ( $\rho=2.97 \text{ g/cm}^3$ ). At least 300 translucent grains were counted to obtain a reasonable average. Analysis of several crystal particles was performed with scanning electron microscope (SEM) and microprobe analysis.

Additionally, tephra particles were isolated during these separation steps from some samples (taken from 1.50, 2.20, 2.80 m under SSE) and analyzed with INAA.

### Results and discussion

The “Stalagmite Profile” (A) and “Main Profile” (B) in Charkadio Cave offer five different lithostratigraphic sections, which are described as follows (see also Fig. 2, which offers a summary of all results of this study):

#### *Dwarf elephant zone (A+B):*

The top section from 0.0 to approximately 3.6 m depth under SSE consists of fine-grained, stratified, bright brown to gray colored gravelly silty sands. The composition of the profile of this section in Fig. 2 shows a discontinuity, indicating the overlap of the Main Profile (B) and the Stalagmite Profile (A). This section is rich in fossil elephant bones, which were found regularly during sampling. XRD analyses showed a mineralogical composition of the sediment consisting of quartz ( $\text{SiO}_2$ ) and feldspars in the whole section. Especially the upper part of this lithostratigraphic layer in A (0.0–1.80 m under SSE) is relatively enriched in calcite ( $\text{CaCO}_3$ ), whereas in the layers (in B) below (1.4–3.60 m under SSE), calcite is missing. These layers contain volcanic ash grains and small pumice fragments (Fig. 2). The tephra grains were analyzed with INAA to identify the volcanic source. Although their mass was very low (8–48 mg), they could be correlated to Kos Plateau Tuff (KPT).<sup>29</sup>

Regarding the noticeable differences in the content of calcite, it can be assumed that the acidic rain during and right after a volcanic event caused dissolution of

CaCO<sub>3</sub>. There is good correlation between the existence of pumice fragments (and thus strata influenced by volcanic activity) and the lack of calcite.

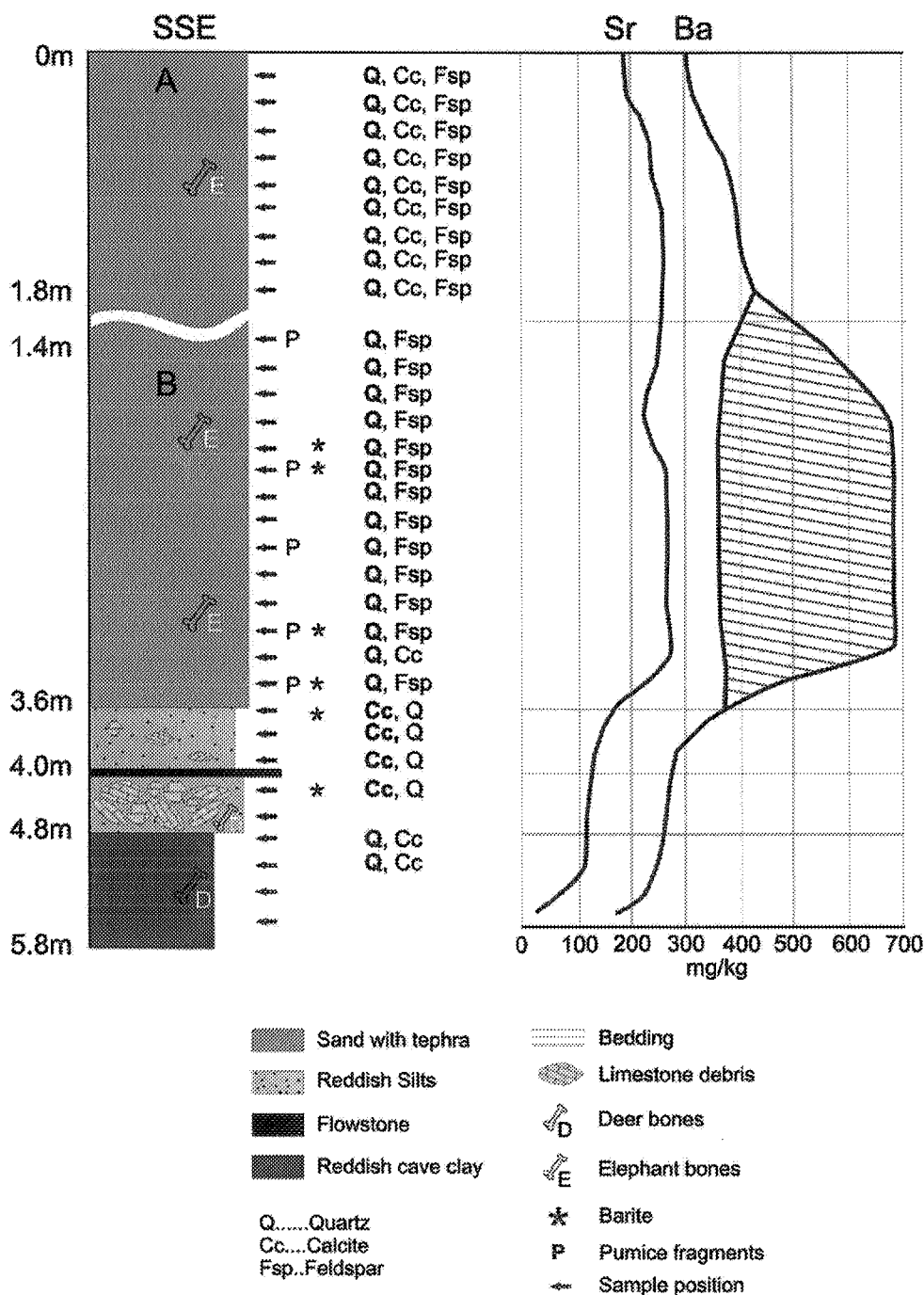


Fig. 2. Composite profiles A and B of Charkadio Cave, including a summary of the results of INAA and mineralogical XRD investigation. The discontinuity stands for the overlap of the two profiles in the cave that have been sampled. INAA- and XRD-data in table form are available on request from the authors

Additionally to this fact, there is a coincidence between the occurrence of volcanic tephra particles and the content of Sr and Ba, as shown in Fig. 2. Those layers influenced by volcanic products show a significant increase in their Sr- and Ba-values compared to the sections without any volcanic activity. The shaded area in Fig. 2 represents the variation (minimum and maximum concentrations) in the Ba content, which is noticeable. Each layer of very high Ba bulk concentrations is followed by a layer which contains a high amount of recrystallized, sometimes even macroscopic barite (Fig. 3). Their delicate hedgehog-like shape indicates an on-the-spot formation in the sediments from aqueous solutions. Therefore, they cannot be a solution residue of weathered limestone or imported together with the allochthonous sediments. The crystals contain 0.6–3.9% SrO (microprobe analysis).

In general, heavy mineral data are dominated by pyroxenes, apatite and amphiboles (brownish to greenish hornblende). A minor component is zircon. In the barite-containing samples, the amount of apatite was found to be smaller than in samples without barite. The highest amount of barite has been found in the lower parts of this lithostratigraphic section.

#### *Transition zone (B)*

The second section (3.6–4.0 m under SSE) above the characteristic sinter layer consists of reddish silts with embedded small limestone fragments. This section contains a zone that is rich in secondary barite crystals. In contrast to the overlaying sediments, the

mineralogical investigation showed the occurrence of calcite, whereas feldspar is missing. This section, like all deeper sections, does not contain significant amounts of pumice fragments. Since feldspar in these sediments is released from weathered pumice only, there is good agreement between the several mineralogical results, evidencing that this section has not been significantly influenced by volcanic activity.

#### *Sinter zone (B)*

The third section is the characteristic horizontal calcite sinter layer ("flowstone") in about 4.0 m under SSE. These cave sediments represent a clear time mark. On the one hand, it is the lower boundary of the occurrence of elephant bones; on the other hand, it is a good indicator for a humid climate and sufficient vegetation on the surface. This calcite sinter layer is supposed to be syngenetic to the big stalagmites (Fig. 1), which have grown under the same climatic conditions. In this stage of development, the cave must have been above groundwater level, lacking of major connections to the surface.

Attempts have been made to date this flowstone:  $^{14}\text{C}$ -dating resulted in an age of  $44900 \pm 2240$  y BP.<sup>3</sup> In 1980, G. J. HENNIG (University of Cologne) performed  $^{230}\text{Th}/^{234}\text{U}$ -dating, which lead to a maximum age of  $107,000 \pm 17000$  y BP ( $\pm 1\sigma$ ). Since radiocarbon dating of flowstone is problematic, the  $^{230}\text{Th}/^{234}\text{U}$ -value appears to be more reliable. The youngest  $^{14}\text{C}$  data for the stalagmites themselves are between about 28,000 and 35,000 y BP (by GEYH).<sup>3</sup>

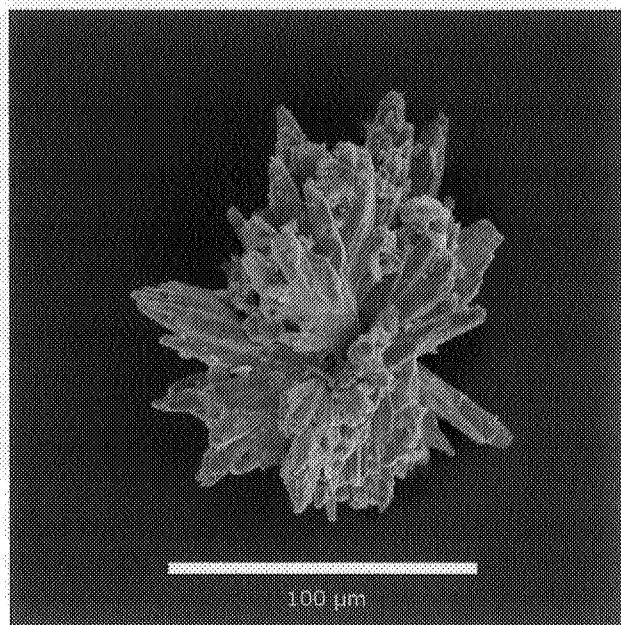


Fig. 3. Scanning electron microscopic picture of a barite crystal from the sediments in Charkadio Cave (Photo by F. BRANDSTÄTTER)

*Collapse zone (B)*

The fourth section (4.0–4.9 m under SSE) consists of large limestone fragments embedded in little reddish, fine-grained sediment. The rock debris from the cave ceiling could be a sign of heavy under-water corrosion and/or earthquake activities. In this time, massive geological changes on Tilos Island must have occurred. In this layer, only few deer bones were found. They were dated with  $^{230}\text{Th}/^{234}\text{U}$  by HILLE and WILD to an age of  $140,000 \pm 11,400$ ,  $-10,200$  y BP.<sup>5</sup> In the upper strata of this zone secondary barite crystals were found.

*Cave clay zone (B)*

The fifth and at the moment basic sediment sequence of the "Main Profile" (4.9–5.8 m under SSE) consists of red fine-grained sediments typical for a deposit in karst caves under ground-water level. Some fossil deer bones are embedded. The mineralogical investigations show only traces of indications of volcanic activity, coinciding with the chemical analyses of these sediments, showing much lower Ba and Sr contents than the sections above.

In general, grain size analyses show an upward coarsening trend for the whole profile, consisting of fine grained clayey silts in the lowest parts of the lithostratigraphic section followed by gravelly sandy silts in the upper parts.

The sediments of the Spider Cave on Tilos were analyzed with INAA, showing significantly lower values for Ba (49 mg/kg) and Sr (63 mg/kg). They are comparable to the Sr- and Ba-content of the "Cave Clay Zone" of Charkadio Cave. Since the Spider Cave was closed until the recent road constructions and has, therefore, not been exposed to any volcanic products, these results strengthen the theory that Ba and Sr anomalies can occur in the course of volcanic activity. This fact requires the existence of mobile Sr and Ba compounds on the surface of the tephra particles or is a result of the weathering of feldspars, which are set free by decaying pumice.

INAA- and XRD-data in table form are available on request from the authors.

**Conclusions**

The mineralogical and chemical analyses of the sediments of Charkadio Cave on Tilos offer new insight to the impact of volcanic eruptions on the composition of a stratified sediment. Increased Ba and Sr values in the sediments of Charkadio Cave were found to coincide clearly with volcanic activity. Thus Ba and Sr concentration anomalies can be regarded as a suitable marker for volcanic eruptions, at least in the Mediterranean. This chemical observation coincides

with the mineralogical analyses (absence of calcite and occurrence of feldspar in sections with volcanic activity).

The increase of Sr- and Ba-values in the sediments requires the either existence of mobile and water soluble compounds on the surface of tephra or the weathering of Sr- and Ba-rich feldspar to be explained. Sr and Ba in the volcanic glass matrix are definitely not mobile enough to cause such anomalies in the surrounding sediment. It can be assumed that volatile Sr and Ba compounds are exhaled in the plume of the volcano during the eruption and adsorbed on the surface of the tephra particles in the cooler regions of the eruption cloud.<sup>26,30</sup> These compounds may be washed from the tephra surface by the acidic rain following the eruption.

As recently shown by STERBA et al.,<sup>27</sup> sulfuric acid decreases the mobility and leachability of adsorbed  $\text{Ba}^{2+}$  on tephra due to the formation of insoluble  $\text{BaSO}_4$ . Following these results, it can be supposed that not the entity of  $\text{Ba}^{2+}$  on the tephra surface existed in the form of  $\text{BaSO}_4$ . In the case of Charkadio Cave, the mobile  $\text{Ba}^{2+}$  and  $\text{Sr}^{2+}$  compounds (most likely chlorides or oxides) might have been leached from the tephra surface by the acidic rain flooding the cave and percolated through the sediments, where the acid was neutralized by the calcite component. With neutralization, precipitation of  $\text{Ba}^{2+}$  and  $\text{Sr}^{2+}$  was induced, leading to typical hedgehog-like shaped barite crystals.

A spontaneous increase of Sr- and Ba-values in a sediment induced by a certain eruption may help dating the respective stratum. In case of Charkadio Cave, we hope to date bones found in a stratum that is too old for  $^{14}\text{C}$  dating by means of the KPT eruption that occurred 161 ky BP.<sup>28</sup>

The investigation of the cave sediments leads further to the conclusion that in earlier days the cave did not have a broad entrance like today. In this case, the cave would have been filled with pure volcanic material to the top, because the present entrance opens towards Nisyros Volcano. The present situation rather suggests a small, cleft-like steep entry leading to the top of the hill. Such a narrow connection would drastically reduce the volume of material entering the cave per time unit. Only water, soil, pumice fragments, potsherds and mostly single bones from the surface of the hill were washed into the cave part by part, while massive pyroclastic flows first obstructed the entrance, which was reopened when the majority of loose tephra already had been washed down to the lower parts of the island.

In the frame of this study, further investigations will also cover the huge tephra deposits on the surface of Tilos Islands and the corresponding deposits on Nisyros Volcano itself. This will provide an insight in this complex scientific field.

\*

This work is supported financially by SCIEM2000, a Special Research Programme of the Austrian Academy of Sciences and the Austrian Science Fund. Further financial support for field work and sample preparation was provided by the ERMANN Fond, Austria. The authors wish to thank R. BACHOFNER and K. BREITENECKER for help with sampling and sample preparation. G. J. HENNIG is acknowledged for the  $^{230}\text{Th}/^{234}\text{U}$  dating of the calcite sinter, F. BRANDSTÄTTER for SEM and microprobe analyses, and V. HAMMER for XRD analyses.

## References

1. N. SYMEONIDIS, *Ann. Géol. d. Pays Hellén.*, 24 (1972) 445.
2. N. SYMEONIDIS, F. BACHMAYER, H. ZAPFE, *Ann. Naturhistor. Mus. Wien*, 77 (1973) 133.
3. F. BACHMAYER, N. SYMEONIDIS, R. SEEMANN, H. ZAPFE, *Ann. Naturhistor. Mus. Wien*, 80 (1976) 113.
4. F. BACHMAYER, N. SYMEONIDIS, *Ann. Géol. d. Pays Hellén.*, 26 (1975) 320.
5. F. BACHMAYER, N. SYMEONIDIS, H. ZAPFE, *Aus den Sitzungsberichten der Österr. Akademie der Wissenschaften, Mathem.-naturw. Kl., Abt. I*, 193/6-10, 1984, p. 321.
6. G. E. THEODOROU, N. K. SYMEONIDIS, in: *The World of Elephants*, G. CAVARRETTA, P. GIOIA, M. MUSSI, M. R. PALOMBO (Eds), *Proc. 2nd Intern. Congress, Comune di Roma, Consiglio Nazionale delle Ricerche, Rome, 2001*, p. 514.
7. G. MARINOS, N. SYMEONIDIS, *Ann. Géol. d. Pays Hellén.*, 28 (1976) 352.
8. P. BROWN, T. SUTIKNA, M. MORWOOD, R. SOEJONO, R. JATMIKO, E. SAPTOMO, R. DUE, *Nature*, 431 (2004) 1055.
9. R. D. GUTHRIE, *Nature*, 429 (2004) 746.
10. A. LISTER, *Nature*, 342 (1989) 539.
11. M. MASSETI, in: *The world of Elephants*, G. CAVARRETTA, P. GIOIA, M. MUSSI, M. R. PALOMBO (Eds), *Proc. 2nd Intern. Congress, Comune di Roma, Consiglio Nazionale delle Ricerche, Rome, 2001*, p. 402.
12. G. STEINHAUSER, J. H. STERBA, M. BICHLER, H. HUBER, *Appl. Geochem.*, 21, 1362.
13. S. THORARINSSON, *Tefrokronologiska Studier på Island*, Munksgaard, København, 1944.
14. S. THORARINSSON, *Tephra studies and tephrochronology: A historical review with special reference to Iceland*, in: *Tephra Studies*, S. SELF, R. S. J. SPARKS (Eds), Reidel, Dordrecht, 1981, p. 1.
15. T. EINARSSON, *Tephrochronology*, in: *Handbook of Holocene Palaeoecology and Palaeohydrology*, B. E. BERGLUND (Ed), John Wiley and Sons, Chichester, 1986, p. 392.
16. J. KELLER, T. REHREN, E. STADLBAUER, in: *Thera and the Aegean World III*, Vol. 2, D. A. HARDY, J. KELLER, V. P. GALANOPOULOS, N. C. FLEMMING, T. H. DRUITT (Eds), 1990, p. 13.
17. V. JACOBSSHAGEN, *Geologie von Griechenland*, Gebrüder Borntraeger, Berlin 1986, p. 363.
18. S. R. ALLEN, E. STADLBAUER, J. KELLER, *J. Earth Sci.*, 88 (1999) 132.
19. M. BOHLA, J. KELLER, *Terra Cognita*, 7 (1987) 171.
20. E. N. DAVIS, *Geol. Rundsch.*, 57 (1968) 811.
21. M. D. HIGGINS, R. HIGGINS, *A Geological Companion to Greece and the Aegean*, Duckworth, London, 1996, p. 240.
22. C. PELTZ, C. SCHMID, M. BICHLER, *J. Radioanal. Nucl. Chem.*, 242 (1999) 361.
23. G. STEINHAUSER, M. BICHLER, G. EIGELREITER, A. TISCHNER, *J. Radioanal. Nucl. Chem.*, 267 (2006) 3.
24. G. P. WESTPHAL, *J. Radioanal. Nucl. Chem.*, 70 (1982) 387.
25. G. P. WESTPHAL, G. R. CADEK, N. KERÖ, T. SAUTER, P. C. THORWARTL, *J. Radioanal. Nucl. Chem.*, 193 (1995) 81.
26. S. MOUNE, P.-J. GAUTHIER, S. R. GISLASON, O. SIGMARSSON, *Geochim. Cosmochim. Acta*, 70 (2006) 461.
27. J. H. STERBA, G. STEINHAUSER, M. BICHLER, *J. Radioanal. Nucl. Chem.*, 276 (2008) 175.
28. P. E. SMITH, D. YORK, Y. CHEN, N. M. EVENSEN, *Geophys. Res. Lett.*, 23 (1996) 3047.
29. G. STEINHAUSER, J. H. STERBA, M. BICHLER, *Appl. Radiation Isotopes*, 65 (2007) 488.
30. G. STEINHAUSER, M. BICHLER, *Appl. Radiation Isotopes*, in press, DOI: 10.1016/j.apradiso.2007.07.010.